Effect of Water Droplets Crossing the Boundary Layer in a Stagnation Point Configuration

Mario Vargas[1]
NASA Glenn Research Center, Cleveland, Ohio, 44135, USA

Stephen T. McClain [2]
Baylor University, Waco, Texas, 76798, USA

Emilio Borges [3]
NASA Glenn Research Center, Cleveland, Ohio, 44135, USA

Andy P. Broeren [4]
NASA Glenn Research Center, Cleveland, Ohio, 44135, USA

An experimental study was conducted in the Vertical Icing Studies Tunnel at the Icing Physics Flow Laboratory of NASA Glenn Research Center to study the effect of water droplets crossing the boundary layer in a stagnation point configuration. The objective of the experiment was to determine if water droplets crossing a boundary layer create turbulent spots that accelerate the boundary layer transition from laminar to turbulent. Water droplets that crossed the boundary layer were generated with a nozzle installed in the plenum. The turbulence level in the boundary layer was measured with a hot wire system when the nozzle was off, air on, and air and water on. The results indicate that the presence of the nozzle alone did not affect the boundary layer. The activation of the nozzle to eject air only or to generate water droplets affected the turbulence level in the boundary layer. The continued study of this effect is needed because of its implications in the development of heat transfer models for icing codes.

I. Nomenclature

k	=	stretch rate constant
u, v	=	components of two-dimensional inviscid flow velocity
u_{bar}	=	average air velocity
$u(t)$	=	air velocity at a given time t
$u'(t)$	=	the Root-Mean-Square (RMS) of the turbulent velocity fluctuations at a particular location over a specified period of time

[1] Aerospace Engineer, Icing Branch, 21000 Brookpark Rd., MS 11-2, AIAA Associate Fellow.
[2] Professor, Department of Mechanical Engineering, One Bear Place #97356, AIAA Associate Fellow.
[3] Aerospace Engineer, Icing Branch, 21000 Brookpark Rd., MS 11-2.
[4] Aerospace Engineer, Icing Branch, 21000 Brookpark Rd., MS 11-2, AIAA Associate Fellow.

II. Introduction

An experimental study was conducted in the Vertical Icing Studies Tunnel (VIST) at the Icing Physics Flow Laboratory of NASA Glenn Research Center to study the effect of water droplets crossing the boundary layer in a stagnation point configuration. The experiment is part of NASA efforts to study the physics involved in ice accretion formations to improve the heat transfer models in the NASA ice accretion codes.

The objective of the experiment was to determine the validity of the following hypothesis in a stagnation point configuration: water droplets crossing a boundary layer will create turbulent spots that will accelerate the boundary layer transition from laminar to turbulent. Understanding of this effect is needed because during the first seconds of an ice accretion encounter, before any ice or roughness elements are formed, supercooled water droplets cross the boundary layer [1] and may accelerate the transition from laminar to turbulent [2]. This physical mechanism may need to be considered when modeling ice accretion formation on the control surfaces of an aircraft in an icing encounter.

To study the effect of droplets crossing the boundary layer, a stagnation point configuration is convenient. In a stagnation point configuration, the boundary layer thickness is constant and laminar. A theoretical calculation of the boundary layer size can be performed and allows the determination of the feasibility of probing its state with a hot wire anemometer. For those reasons, the experiment was conducted in the Vertical Icing Studies Tunnel at NASA Glenn Research Center which is a scaled version of the area around the stagnation point of a NACA 0012 airfoil.

This first study is a work in progress. There were limitations in the control and variation of some parameters which will be discussed in a section of this paper. Despite those limitations, the results show the importance of doing additional work in this area to gain understanding of the physics in the first seconds of an icing encounter, and help icing code developers reach a better understanding of the assumptions in the modeling of the icing phenomena.

III. Conceptual View of the Experiment

Figure 1 shows the conceptual view of the experiment. The tunnel is set at given velocity. A boundary layer is generated along the plate. A nozzle located in the plenum generates water droplets that cross the boundary layer. The state of the boundary layer is probed with a hot wire anemometer. The droplets ejected by the nozzle are created by the interaction between a water jet and air flow. The water and air are brought to the nozzle by separate tubes and are mixed in the nozzle head. The instabilities in the water jet created by air flow generate the water droplets. The nozzle can be operated with air only (no droplets), or with water and air to generate the droplets. When operated with air only, the ejected air from the nozzle can potentially create turbulence in the plate boundary layer. When the nozzle is not being operated, its presence alone in the plenum may potentially create turbulence at the plate. To study the effect of the presence of the nozzle, the air flowing from the nozzle, and the water droplets on the state of the boundary layer, the hot wire was operated in a specific sequence. That sequence probed the state of the boundary layer with the nozzle off, with air flowing through the nozzle, and with water droplets ejected from the nozzle.

IV. Experimental Method

The experiment was conducted in the stagnation point test section of the VIST. The test section is a scaled version of the area around the stagnation point of a NACA 0012 airfoil. The large size of the diffuser and plate that form the

stagnation point configuration allowed for the installation of a nozzle in the plenum ahead of the diffuser. The nozzle generated the drops that crossed the boundary layer. The air velocity in the tunnel could be varied from 4.6 m/s (15 ft/sec) to 16.8 m/s (55 ft/s). A hot wire system was used to probe the state of the boundary layer. The hot wire system could be located at four different positions along and above the plate. The main advantage of the stagnation point configuration is that the laminar boundary layer remains constant in height along the plate. A theoretical calculation of the boundary layer size is possible and allows to determine the feasibility of probing its state with a hot wire anemometer.

The air velocity in the tunnel was measured at the top of the diffuser and at the throat, where the contraction is at its minimum value. The throat velocity was varied from 4.6 m/s (15 ft/sec) to 16.8 m/s (55 ft/s). The hot wire system was moved vertically and programed to follow a specific path in and out of the expected boundary layer. With the tunnel set at a given velocity, three scenarios were studied for the activation of the nozzle: initially the nozzle was turned off, then the nozzle air was turned on and finally the full nozzle was activated. For each scenario, the hot wire probed the boundary layer twice. Beginning above the boundary layer it traveled down to a point as close as possible to the plate and then moved back to the original starting location. The probing of the boundary layer with the nozzle ejecting air only was done to separate the effect of the air from the droplets. The data from the hot wire was saved to an Excel file. A MATLAB program was developed to calculate the variation in the velocity with respect to the average velocity. The program was also used to calculate the Fast Fourier Transform to obtain the velocity frequency spectrum.

V. Experimental Setup

A. The Vertical Icing Studies Tunnel

The experiment was conducted in the Vertical Icing Studies Tunnel at the Icing Physics Flow Laboratory of NASA Glenn Research Center (Fig. 2). The VIST is a closed-loop vertical tunnel. Figure 3 is a diagram of the tunnel showing the flow path and vertical layout. A 3 hp, 1750 rpm, DC motor moves the air in a counterclockwise direction. The air flows vertically through a heat exchanger before encountering the first ninety-degree corner. The corner is equipped with a set of turning vanes. The air flows horizontally to the next ninety-degree corner. The turning vanes in this second corner direct the air downward into the plenum and towards the contraction. Before the contraction, the air flows through a honeycomb section and a series of stainless-steel screens designed to reduce the free stream turbulence and improve mean-flow uniformity. After the screens, the air flows through the contraction, the throat and then the test section. The contraction ratio is 7.2 to 1. The throat is 100 mm (4 inches) wide. The velocities at the throat range from 2 m/sec (6.5 ft/sec) to 25 m/sec (82 ft/sec).

The test section (Fig. 4 and 5) was designed to simulate stagnation point flow [3-8]. The diffuser is located after the throat and directs the flow over a flat plate. The walls of the diffuser were designed to follow the streamline of two-dimensional inviscid stagnation point flow over the flat plate. The shape of the diffuser walls in the original design was given by y=60/x, with x varying from 50 mm (2 inches) to 750 mm (30 inches). However, the shape of the walls has since been redesigned to avoid flow separation. The improvement in the flow quality has been verified with pressure measurements along the plate, and flow visualization on the walls.

The height of the diffuser is 750 mm (30 inches). The plate is 1500 mm (60 inches) wide, centered at 750 mm (30 inches) from the center line to its edge. At the end of the diffuser, the tunnel wall has a curved shape (half of a circle) to guide the flow over the plate edges and below the plate. From there the air flow is directed horizontally towards the motor intake completing a full loop around the tunnel.

The test section size was designed to achieve two requirements. The first requirement was to maintain a 2 mm (0.079 inch) boundary layer thickness along the plate. The second was to achieve a boundary layer Reynolds number equivalent to a wing chord-based Reynolds of $10x10^6$. To fulfill those two requirements the total length of the plate needed to be 1500 mm across (two symmetric sides, 750 mm each). The two requirements dictated that the stretch rate k have a value of 23 s^{-1}. The stretch rate is the constant used to calculate the stagnation point flow inviscid velocities $u = k \cdot x$ and $v = -k \cdot y$. The two requirements were fulfilled for tunnel velocities of 4.6 m/s (15 ft/sec) to 16.8 m/s (55 ft/s).

B. The Nozzle System

To generate the water droplets, a nozzle was installed in the plenum after the honeycomb section and the stainless-steel screens. It was positioned at a middle point with respect to the tunnel walls in a cage at the end of a rod (Fig. 6 and 7). The operation of the nozzle required a water line and two pressure lines. The water line and one pressure line were needed to generate the droplets. The other pressure line operated a needle that acted as an on-off valve for the water and pressure lines that generate the droplets in the head of the nozzle. The rod, the air and water lines were supported at the wall of the tunnel with a clear plastic window.

The air source was shop air. The air pressure was controlled with computer operated TESCOM pressure regulators. The water flow and pressure were controlled with a water tank system (Fig. 8). The nozzle was operated at preset water and air pressures that generated a plume of water droplets (Fig. 9). The distribution and/or the mean volumetric diameter of water drops was not controlled. Optical measurement of the drop sizes showed a range of values with most of the drop diameters near 150 micrometers. The plume of droplets had a flat fan shape that minimized the contact of the water with the walls of the test section.

C. Hot Wire System

A TSI IFA 300 constant temperature anemometer system was used to probe the state of the boundary layer with a hot wire. The hot wire was mounted on a computer-controlled positioning system (Fig. 10). This system allowed accurate positioning of the hot wire along a specific sequence of locations. The hot wire positioning system could be located at any one of four access ports in the diffuser of the test section (Fig. 11). This allowed probing the boundary layer at four different locations along the plate. During operation, at a given position, the hot wire probed the flow at a sampling rate of 25,000 Hz or 50,000 Hz.

Several probes were tried with the hot wire system and data was taken with each of them. Because water contamination occurs after the probe is exposed to the water drops, most of them were discarded. The probe that provided the best data was a TSI 1261-10 (Fig. 12). The shape of the probe allowed 90 seconds before it became contaminated. The position sequence was chosen so that the probe was exposed to water droplets less than 90 seconds when probing the boundary layer.

D. Hot Wire Path

A program was developed using the LabVIEW design platform from National Instruments to control the tunnel, the water and air pressures for the operation of the nozzle, the hot wire and its positioning sequence, the hot wire sampling rate, and the saving of the data to a file. The data file format was TDMS (the binary file format developed by National Instruments) and it could be read with Excel. When the hot wire was positioned at one of the four access ports, the flow was probed along a specific path. The path was defined with vertical steps of the hot wire above the plate. Data was taken for several paths, two of which are shown in figures 13 and 14.

The following is a description of the hot wire data taken along the path shown in figure 14. Before the tunnel was started, the vertical control of the hot wire was used to place it as close to the plate as possible. This initial position was considered height 0.00 and step 0. With the tunnel set at a given air velocity and the water nozzle off, the hot wire moved up from its initial height at 0.00 to step 1 at a height of 0.3 inches (7.6 mm). From there it began probing the flow, moving downward. It moved down in 40 steps, at a rate of 0.0075 inches (0.19 mm) per step. At each step it probed the flow for 10 seconds and took 50000 readings of the velocity. When it reached the position 0.00 closest to the plate (step 41) it began moving up. It moved up 14 steps (to step 55) to a height of 0.1050 inches (2.67 mm). When it reached this position, it remained there one step, 10 seconds. During this time, the nozzle air was turned on. At this point the hot wire had probed the boundary layer twice, going from step 1 to 41, and from step 41 to 55. During this trajectory, the probe measured the level of turbulence in the boundary layer due to the tunnel components and the presence of the nozzle.

Next the hot wire moved downward from step 55 to 69, back to height 0.00. From this position it moved up 14 steps (to step 83) to a height of 0.1050 inches (2.67 mm). Then it moved downward from step 83 to 97, back to height 0.00. Between steps 55 and 97 the hot wire probed the boundary layer three times to determine the level of turbulence in the boundary layer due to the activation of the nozzle air.

At step 97 the nozzle water was turned on and the nozzle was fully operational. A plume of water droplets was ejected from the nozzle as shown in figure 9. From step 97 the hot wire moved upward to step 111, at a height of 0.1050 inches (2.67 mm). At step 111 the nozzle was turned off. During steps 97 to 111 the hot wire probed the boundary layer once to determine the level of turbulence in the boundary layer due to the full activation of the nozzle.

In figures 13 and 14, the labels at each position of the hot wire indicate the step number, the time from when the motion of the hot wire began and the vertical distance from the position closer to the plate (given in inches). The position of the hot wire closest to the plate was labeled 0.0 inches. Vertical positions away from the closest position to the plate were specified using negative values. The vertical axis of the graphs is in negative numbers.

E. Measurement Procedure and Processing

For velocities of 15, 20, 25, 30, 35, 40, 50 and 55 feet per second (4.6, 6.1, 7.6, 9.1, 10.7, 12.2, 13.7, 15.2 and 16.8 meters per second) the boundary layer was probed with the hot wire following the path show in figure 14. As the hot wire traversed a path, it measured the velocity u(t) 50000 times at each step. This velocity is a function of time since the 50000 readings are recorded during the time that the hot wire remained at each step (10 seconds per step in figure 14). The u(t) velocity readings at each step were simultaneously sent to a TDMS file. After each run the TDMS file

was opened with Excel and the data was examined. If no problems or errors were found it was stored for post-processing and analysis.

During post-processing, a MATLAB program was used to calculate for each run, at each step along the path, the velocity fluctuation $u'(t)/u_{bar}$, where u'(t) is the instantaneous velocity fluctuation at a particular location and time, over a period of time, and u_{bar} is the average of the velocity over a period of time larger than the period of the velocity fluctuations:

$$u(t) = u_{bar} + u'(t)$$

$$u_{bar} = \frac{1}{T}\int_{t}^{t+T} u(t)dt$$

$u'(t)/u_{bar}$ gives an indication of the turbulence level in the flow. This value is used in figures that will be discussed below. It gives the turbulence level as a percentage.

The MATLAB program also calculated the Fast Fourier Transform (FFT) of the velocity at each step along the hot wire path. In turbulence studies the Fast Fourier transform is typically used to calculate the energy density (energy/unit mass) spectrum of the turbulent fluctuations. In the present work, the Fast Fourier Transforms was used to calculate the distribution of the amplitude of the disturbances (eddies) in the flow against frequency, the amplitude spectrum. At low levels of turbulence, large amplitudes are expected at the lower frequencies (few large disturbances (eddies) in the flow). Smaller amplitudes are expected at the higher frequencies (small disturbances dominate). As the turbulence level increases the larger amplitudes propagate toward the higher frequencies indicating that larger disturbances (eddies) now dominate the flow.

F. Probe Contamination

The main difficulty with the hot wire measurement was the contamination or "flooding" of the probe. When the nozzle was activated, the water droplets in the air collected on the supports of the hot wire and from there ran to the hot wire itself as shown in figure 12. This contamination happened before the actual hot wire was directly flooded by the water drops. Several hot wire configurations were tested to limit contamination from the supports while having enough time to take the measurements. The TSI 1261-10 probe configuration worked best. For this probe, the supports of the hot wire were behind and downstream from it. This allowed for a reasonable time window before the water from the supports contaminated the wire.

The hot wire paths were designed to expose the probe to the least amount of time with the nozzle water on. For the path shown in figure 13, the probe was exposed to the water drops for 134 seconds between step 147 and step 179. During this time, it traversed the boundary layer twice. For the path shown in figure 14, the probe was exposed to the water drops for 140 seconds between step 97 and step 111. During this time, it traversed the boundary layer once. For this path, the water was turned on when the probe was at position 0.00 inches. From there it covered the boundary layer thickness of 2 mm (0.079 inch) in 140 seconds. In all the runs, a side camera recorded the condition of the hot wire.

In addition to the contamination by flooding, the probe reacts to each impact of a water droplet when exposed to a spray. The approach of Henze and Bragg [9] presents a method to remove drop-impact responses from hot-wire bridge signals to assess the turbulence intensity of water droplet laden airflows over wind tunnel models. However, Henze and Bragg only assess turbulence intensity evaluation and not FFT or power spectrum impacts when analyzing hot-wire turbulence characterizations. When removing a drop impact signals from the hot-wire bridge signal to perform the FFT, two options are available: 1) the suspected drop-impact velocity response can be replaced in the signal using the mean velocity or 2) the velocity signal can be truncated to remove the drop-impact event. Replacing the impact signals with the mean velocity keeps the frequency range of the signal consistent, but high and low-frequency noise is introduced by imposing constant regions in the velocity signal. Truncating the signal changes the frequency range and resolution as well as introduces high frequency noise associated with the drop-impact event rate. Consequently, frequency analysis of hot-wire signals with droplet is an active area of research, and the FFT results presented in this paper are of unfiltered velocity signals only.

G. Limitations in the Control of the Experiment

In this preliminary study on the effect of water droplets crossing the boundary layer, it was not possible to vary or control some parameters. The number of drops per unit area per unit time crossing the boundary layer at a given location was not measured. The nozzle air and water pressure were kept at the same values for each run. The assumption was that this would keep the same flux of water droplets for each run at each location along the plate for runs at the same velocity. The experiments were conducted at room temperature and the water droplets were not supercooled. The droplet size measured was in the range of 150 micrometers and the nozzle was operated to keep this drop size. No variation of the droplet size was attempted. The time during which the boundary layer was exposed to air and water droplets (time scale) was kept constant and was not varied during this set of experiments.

VI. Results

For analysis, the data is presented in three plots. The first plot, labeled (a) in figures 15 to 18, shows the vertical position of the hot wire given in inches and is indicated as a red dot in the plot. A second plot labeled (b) shows the velocity fluctuations, u'(t)/ubar, during a one second interval. A third plot labeled (c) shows the amplitude spectra calculated with the FFT. The data analysis program generated a video file in MPEG-4 format with the three plots for each run being updated simultaneously as the hot wire transverse the path. The video could be run all at once or frame by frame. This way of viewing the data allowed clear observation of the state of the boundary layer when the hot wire was traversing it. Figures 15 to 18 are still frames from the mp4 video, when the tunnel velocity was 40 ft/sec (12.2 m/sec) and the hot wire followed the path shown in figure 14.

Figure 15(a) shows the hot wire at a position 0.3 inches above the plate and in the flow outside the boundary layer. Figure 15(b) shows the turbulence level $u'(t)/u_{bar}$. It shows that at this location the turbulence level is within ±5 percent, relatively low. Figure 15(c) shows the amplitude spectrum. Since turbulence level is low, this amplitude spectrum was used as the baseline to gauge the increase in the turbulence level in the boundary layer, as air and water in the nozzle were sequentially activated.

Figure 16(a) shows the hot wire at a position 0.05 inches above the plate and in the boundary layer. Figure 16(b) shows the turbulence level. The turbulence level is within ±5 percent but with some larger spikes in the negative values. Figure 16(c) shows the presence now of larger amplitudes in the frequencies between 10 to 100 hertz. The red line indicates the average values for the FFT amplitudes in the boundary layer measurements with the air and water off. This line is drawn to provide an easy comparison to the cases when the nozzle air and/or water are activated.

Figure 17(a) shows the hot wire at a position 0.05 inches above the plate after it has traversed the boundary layer once and is moving up towards position 0.1050 inches. Figure 17(b) shows a noticeable increase in the turbulence level of the boundary layer as the nozzle air is on. It is now ±10 percent with large spikes in the negative values. There is definite effect on the turbulence level of the flow due to the injection of air from the nozzle. Figure 17(c) confirms this increase in the turbulence level. The gold line represents the average of the amplitude of the FFT results inside the boundary layer with the air activated. This average is above the red line average when the nozzle and water are off. The amplitude of the disturbances (eddies) is larger, and they cover a greater range of frequencies.

Figure 18(a) shows the hot wire at position 0.05 inches above the plate and in the boundary layer after the nozzle air and water were activated. Figure 18(b) shows that the level of turbulence has dramatically increased and is now larger than ±20 percent. The presence of the droplets crossing the boundary layer has affected the level of turbulence in the boundary layer. Figure 18(c) confirms this change. The purple line showing the average values of the amplitude is now above the gold line representing the case where only the nozzle air was activated. The amplitude of the disturbances (eddies) in the boundary layer has not only increased, but now covers the whole frequency range.

The data presented in figures 15 through 18 was taken at a velocity of 40 ft/sec (12.2 m/sec) at position 2 along the plate. A comparison with the state of the boundary layer at position 4, downstream of position 2, and for the same velocity, is presented in Figures 19 through 22. In each figure, the images labeled (a) show the position of the hot wire; images labeled (b) show the state of the boundary layer at position 2; and images labeled (c) show the state of the boundary layer at position 4. Figure 19 compares the state of the flow outside the boundary layer for positions 2 and 4. The level of turbulence is higher at position 4. The same behavior is observed for the boundary layer when the nozzle is off (Fig. 20) and when the air is on (Fig. 21). When air and water are on (Fig. 22), the level of turbulence at both locations is extremely high. This behavior should be expected since the air flow arriving at position 4 is already perturbed upstream.

Figures 23 through 26 compare the effect of increasing the velocity from 40 ft/sec (12.2 m/sec) to 55 ft/sec (15.2 m/sec) for measurements taken at position 2. Only a slight increase in the level of turbulence is observed outside the boundary layer (Fig. 23). The same level of turbulence can be observed when the nozzle is off (Figure 24) and when air is on (Fig. 25). This can be expected since the increase in the velocity did not increase much the level of turbulence in the flow outside the boundary layer. When air and water are on, the level of turbulence for both velocities (Fig. 26) is extremely high. The main effect on the boundary layer is from the water droplets crossing it and the droplets impacting the wire. In this experiment we could not separate the two effects. From figure 26 it is not possible to determine if the increase in velocity increased the level of turbulence in the boundary layer when air and water are on. The turbulence level at both velocities is extremely high.

Since some parameters in the experiment were fixed or not controlled, and additional data from the experiment needs to be analyzed, the results should be taken mainly as guidance for improvement in the experimental configuration, control of the parameters involved in the phenomena, and the employment of a more quantitative method to analyze the hot wire data. But even within the limitations of the experiment, the experimental results strongly suggest that there is a definite effect on the turbulence level in the boundary layer due to the crossing of the water droplets. Additional exploration of the phenomena should be pursued. In particular, a parametric study on the effect of the variables involved should be conducted. Other experimental configurations that allow better control of the experimental parameters should be explored.

VII. Conclusions

An experimental study was conducted in the Vertical Icing Studies Tunnel at the Icing Physics Flow Laboratory of NASA Glenn Research Center to study the effect of water droplets crossing the boundary layer in a stagnation point configuration. The objective of the experiment was to determine if water droplets crossing the boundary layer create turbulent spots that accelerate the transition from laminar to turbulent. The following are the main conclusions from the experimental effort:

- Within the limitations of the experimental configuration and the set of data analyzed, the experimental results suggest that there is an effect on the turbulence level in the boundary layer due to the crossing of the water droplets.
- The experimental results indicate that additional exploration of the phenomena should be pursued with improvements in the experimental configuration, and in the data processing to exclude droplet impacts on the hot wire sensors. With better control of the parameters, a parametric study should be conducted to determine the effect of the variables involved.
- Other experimental configurations different from stagnation point should be explored.

Acknowledgments

The authors would like to thank Dr. Andrew Work, Dr. Mark Potapczuk, Ms. Kristie Elam, Mr. Quentin Schwinn, and Ms. Jordan Salkin for their help and support during the project. The research work was funded by the Advanced Air Transport Technology (AATT) Project.

References

[1] Olsen, W. and Walker, E., “Experimental Evidence for modifying the Current Physical Model for Ice Accretion on Aircraft Surfaces”, NASA-TM-87184, January 1, 1986.

[2] Chen, C. Philip; Goland, Yaccov; and Reshotko, Eli, "Generation Rate of Turbulent Patches in the Laminar Boundary Layer of a Submersible", Published in Viscous Flow Drag Reduction, edited by Gary R. Hough, Vol. 72 of Progress in Astronautics and Aeronautics, 1980.

[3] White, Edward B., "Design and Construction of an Icing Physics Flow Laboratory," FY2004 Grant Proposal to NASA Glenn Research Center from Dept. of Mechanical and Aerospace Engineering, CWRU, Cleveland OH, 2003.

[4] Rabbitt, William E., "The Design and Construction of the Icing Physics Flow Laboratory," M.S. Thesis, Dept. of Mechanical and Aerospace Engineering, CWRU, Cleveland, OH, 2006.

[5] Cebeci, Tuncer and Kafyeke, Fassi, "Aircraft Icing," Annual Review of Fluid Mechanics, Vol. 35:11-21, January 2003, https://doi.org/10.1146/annurev.fluid.35.101101.161217

[6] Gent, R.W., Dart, N.P., and Cansdale, J.T., "Aircraft Icing," Philosophical Transactions of the Royal Society A: Mathematical, Physical and Engineering Sciences, Vol. 358, No. 1776, pp. 2873-2911, Ice and Snow Accretion on Structures, Nov. 15, 2000, https://doi.org/10.1098/rsta.2000.0689

[7] Messinger, Bernard L., "Equilibrium Temperature of an Unheated Icing Surface as a Function of Air Speed," Materials Science, Journal of the Aeronautical Sciences, 1953, https://doi.org/10.2514/8.2520

[8] Reshotko, Eli; Saric, William and Nagib, Hassan, "Flow Quality Issues for Large Wind Tunnels,' AIAA A9715301, Meeting Paper 97-0225, Jan. 1997, https://doi.org/10.2514/6.1997-225

[9] Henze, C.M, and Bragg, M.B., (1999), "Turbulence Intensity Measurement Technique for Use in Icing Wind Tunnels," *Journal of Aircraft*, Vol. 36, No. 3, pp. 577-583.

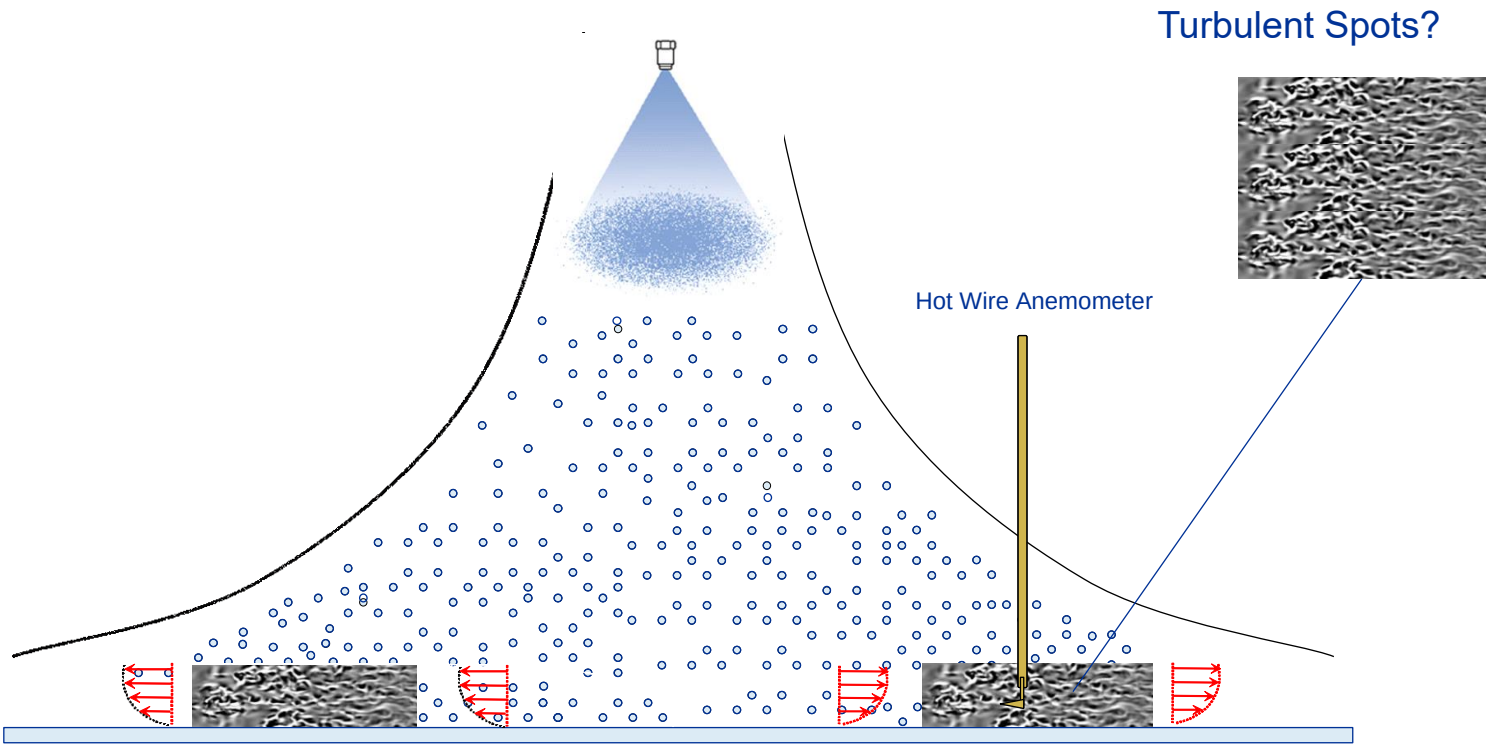

Fig. 1 Conceptual View of Experiment

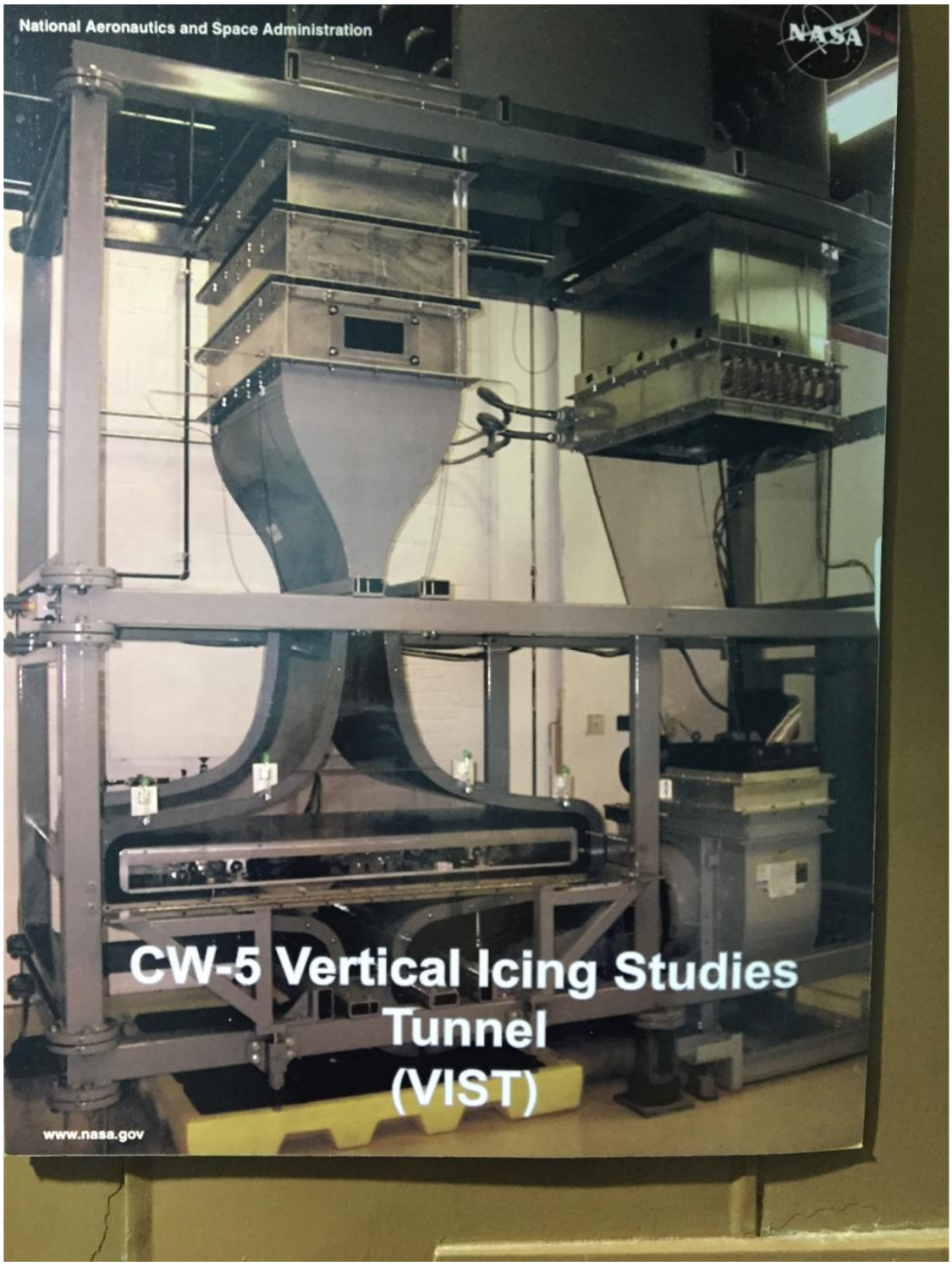

Fig. 2 Vertical Icing Studies Tunnel

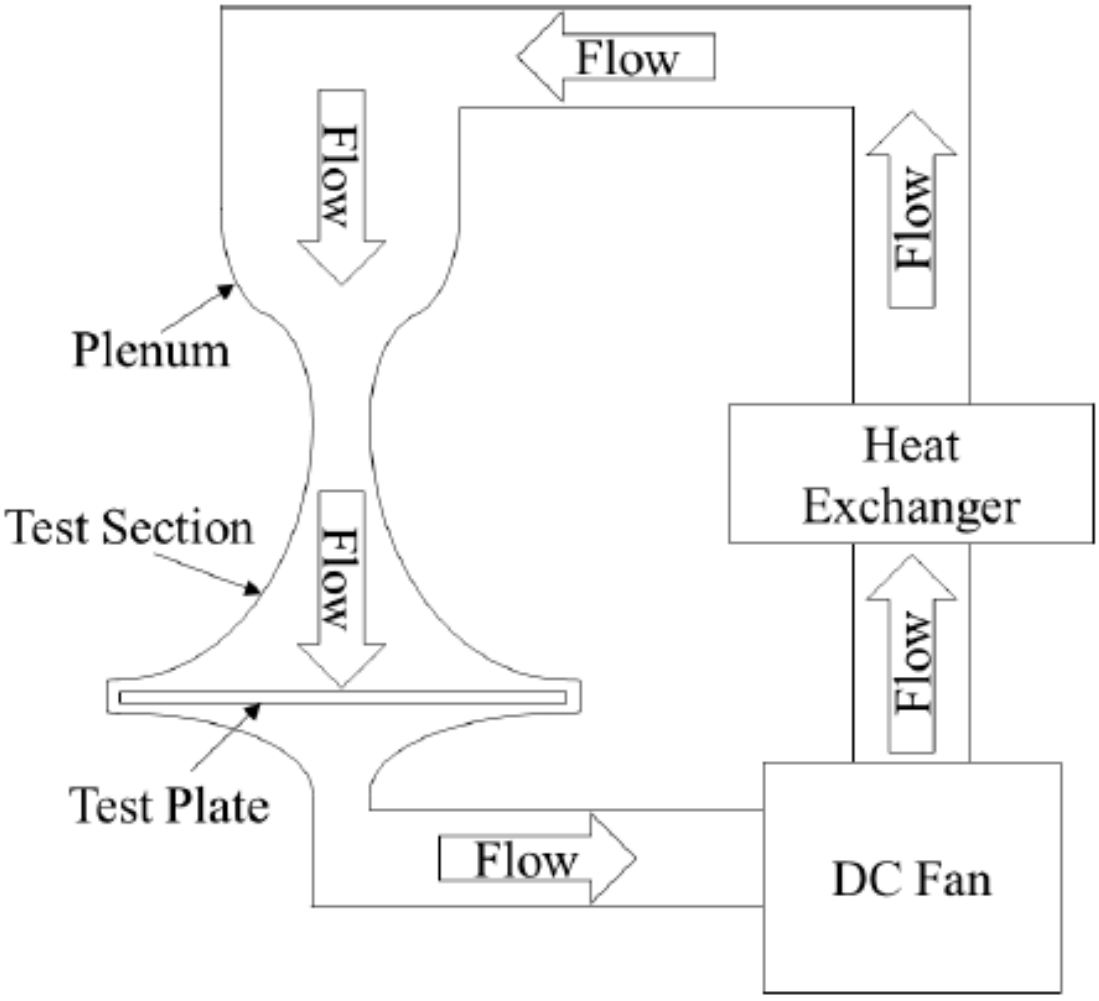

Fig.3 Diagram of the VIST showing the basic flow path and vertical layout

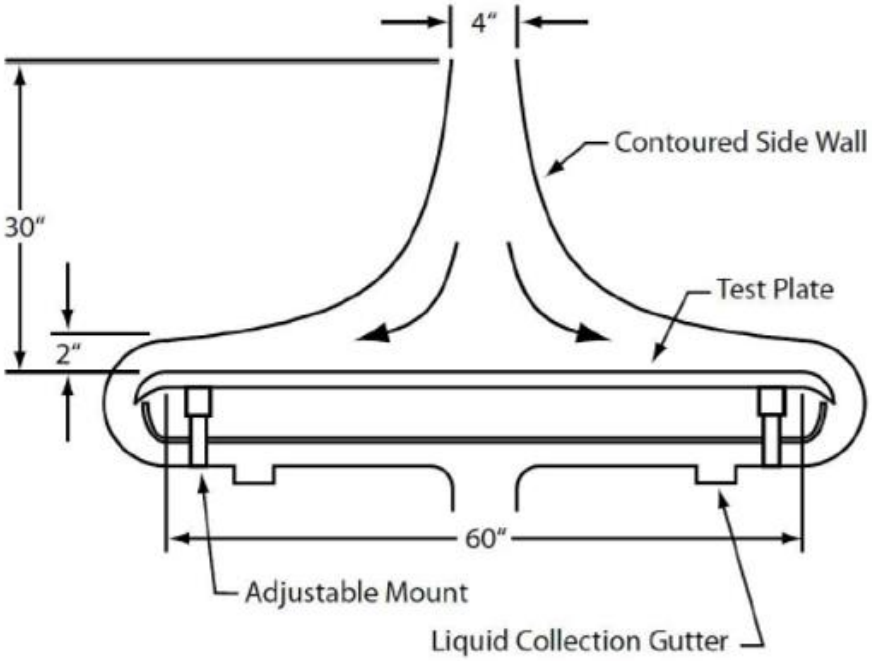

Fig.4 Diagram of Test Section

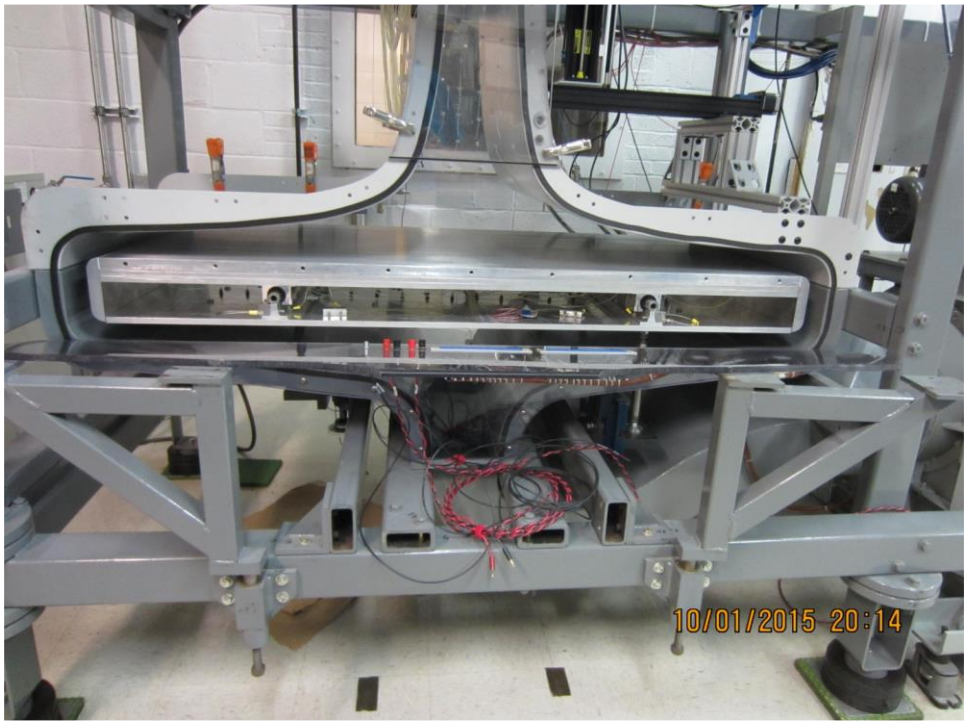

Fig. 5 Test Section

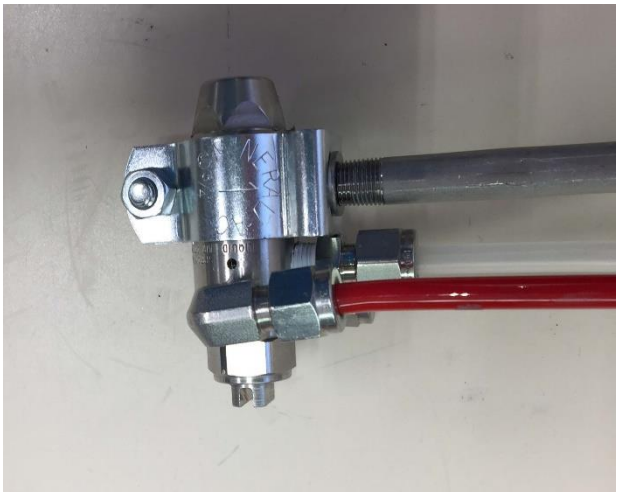

Fig.6 Nozzle

Fig.7 Rod supporting the Nozzle and Window supporting the Rod, and Two Connectors for Air and Water Supply

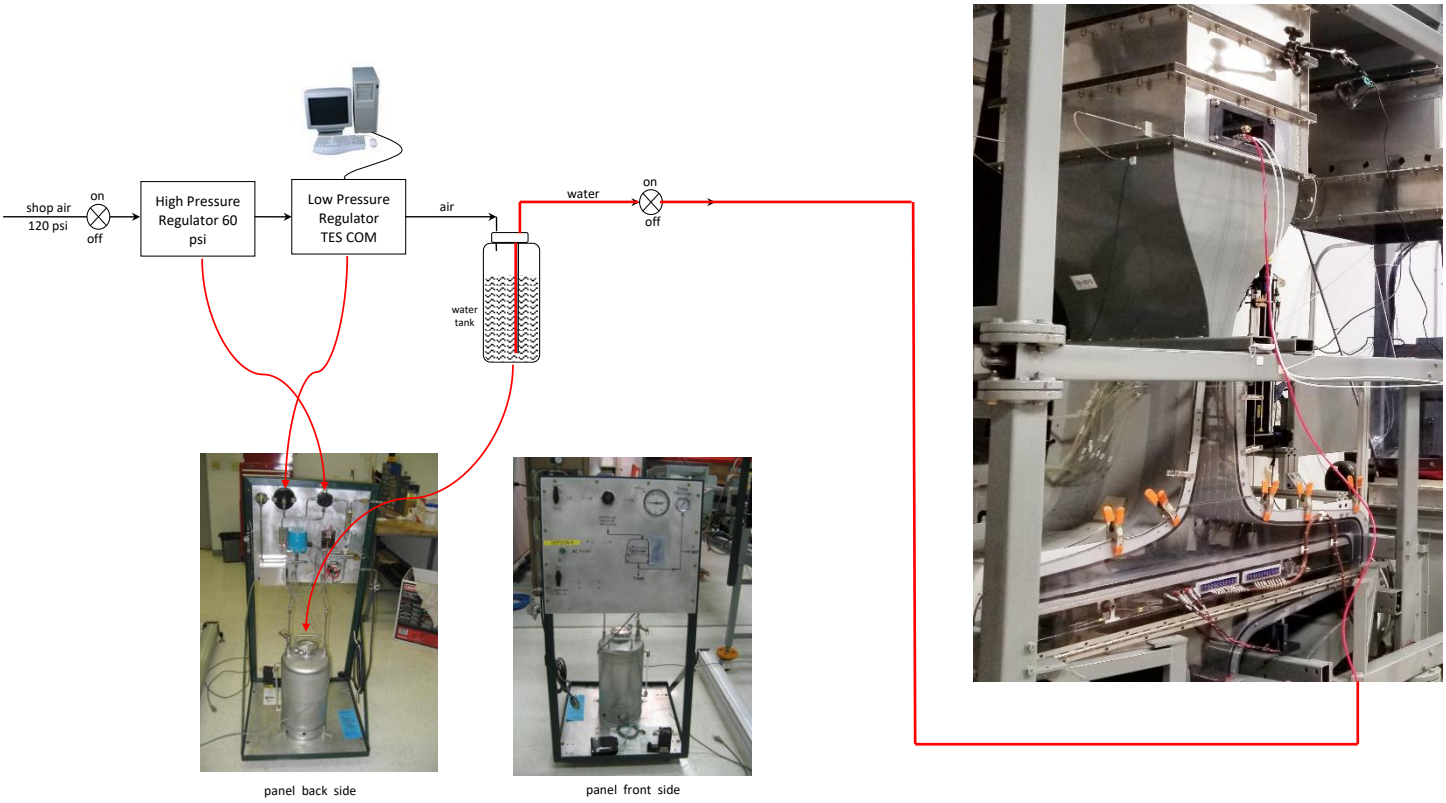

Fig.8 Water Supply System

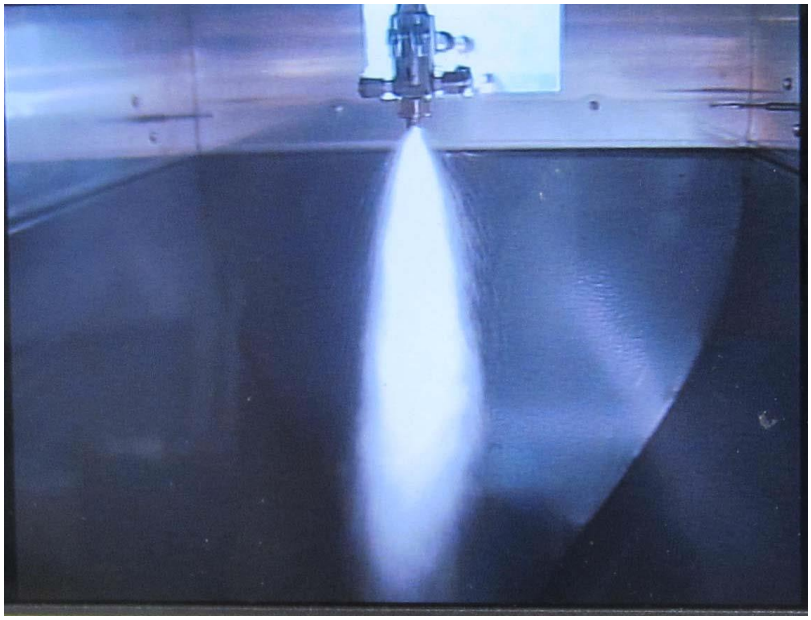

Fig. 9 Nozzle generating a Plume of Water Droplets

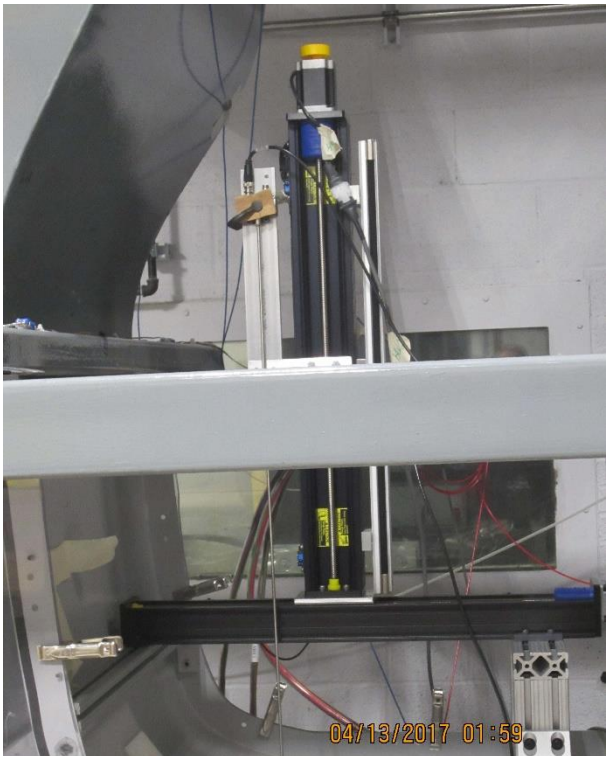

Fig. 10 Hot Wire Positioning System

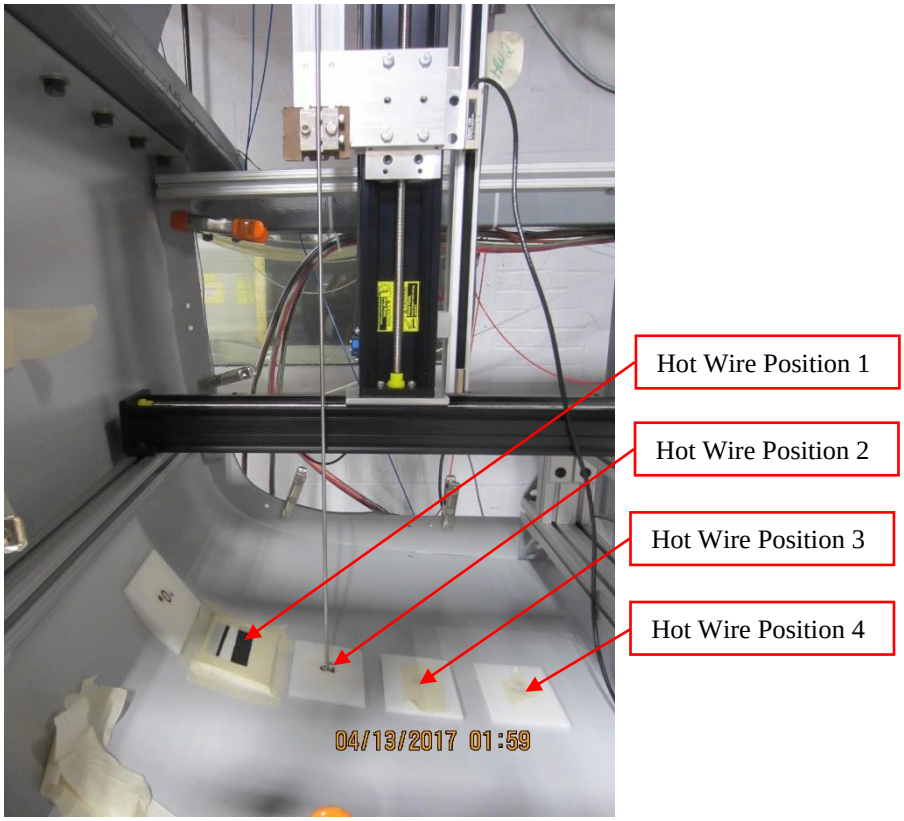

Fig. 11 Four Access Ports and Positions for Hot Wire Measurements

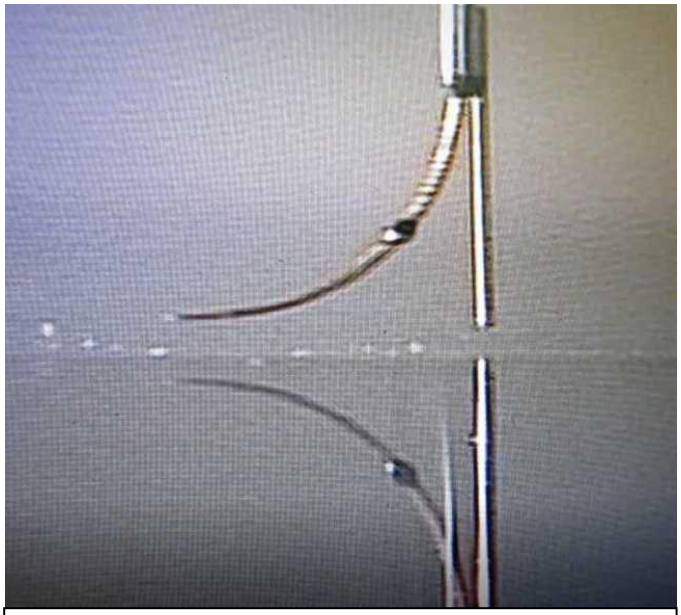

Fig.12 TSI 1261-10 Hot Wire Probe

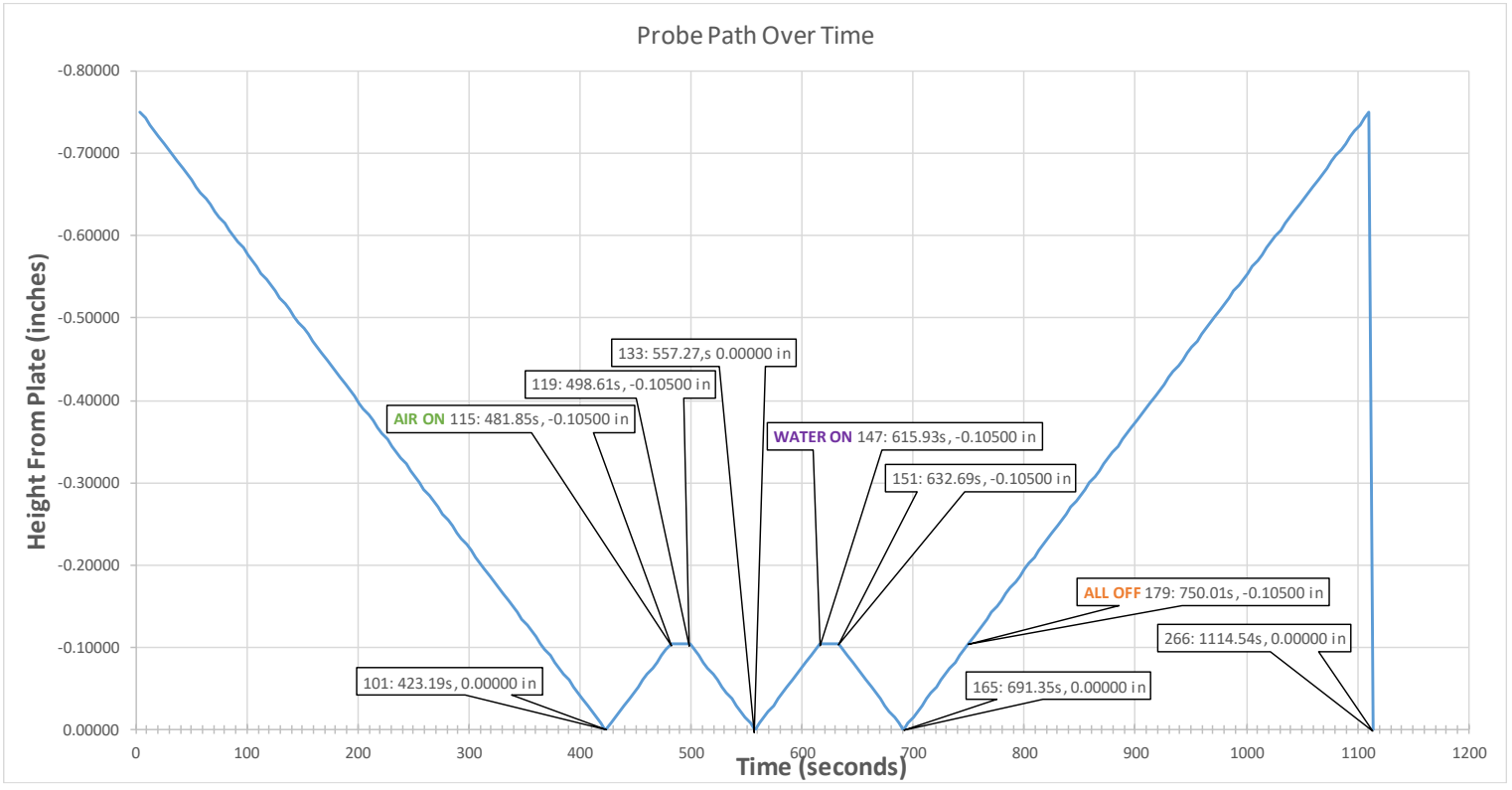

Fig.13 Hot Wire Path

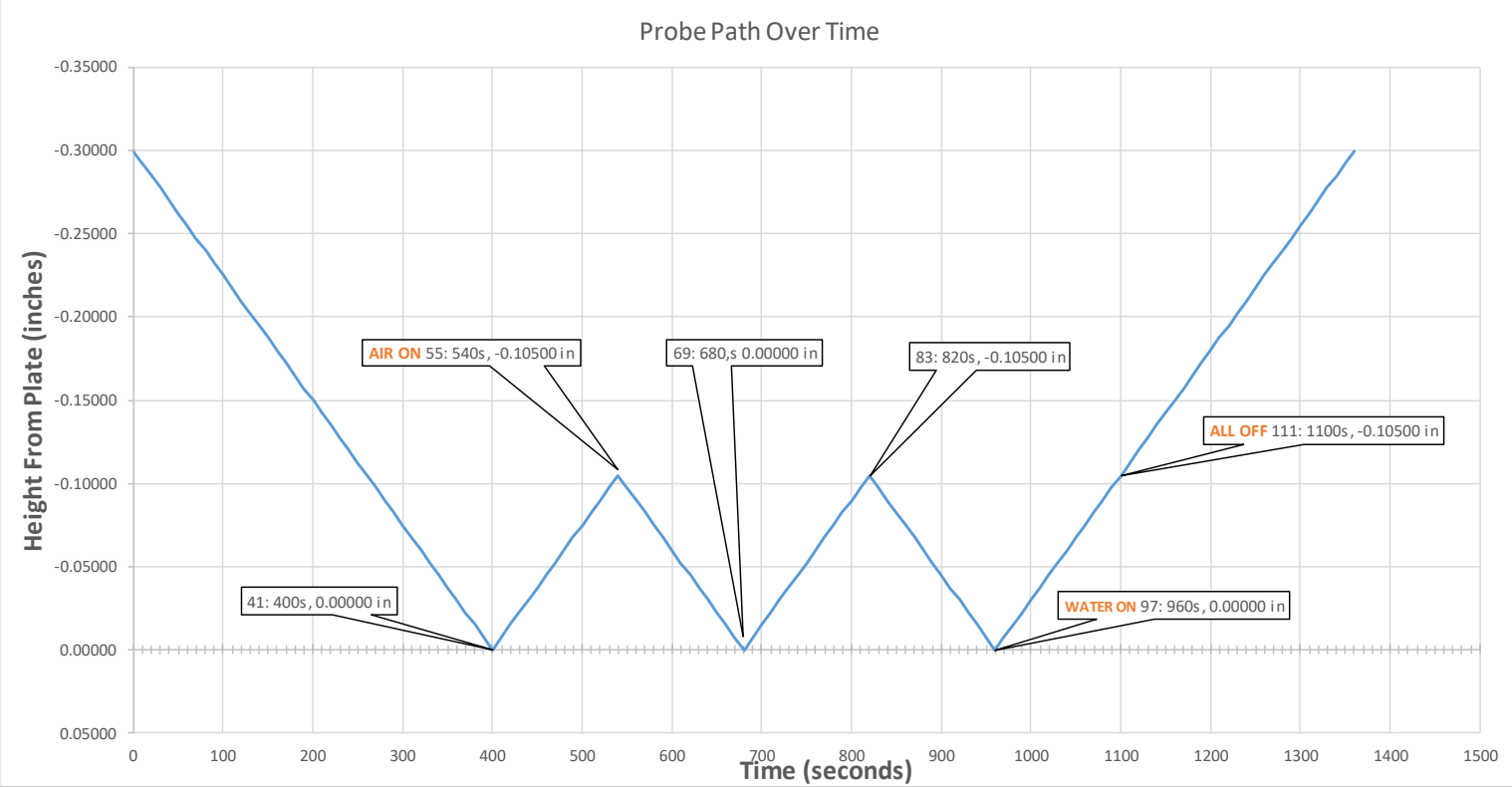

Fig. 14 Hot Wire Path to minimize Probe Contamination

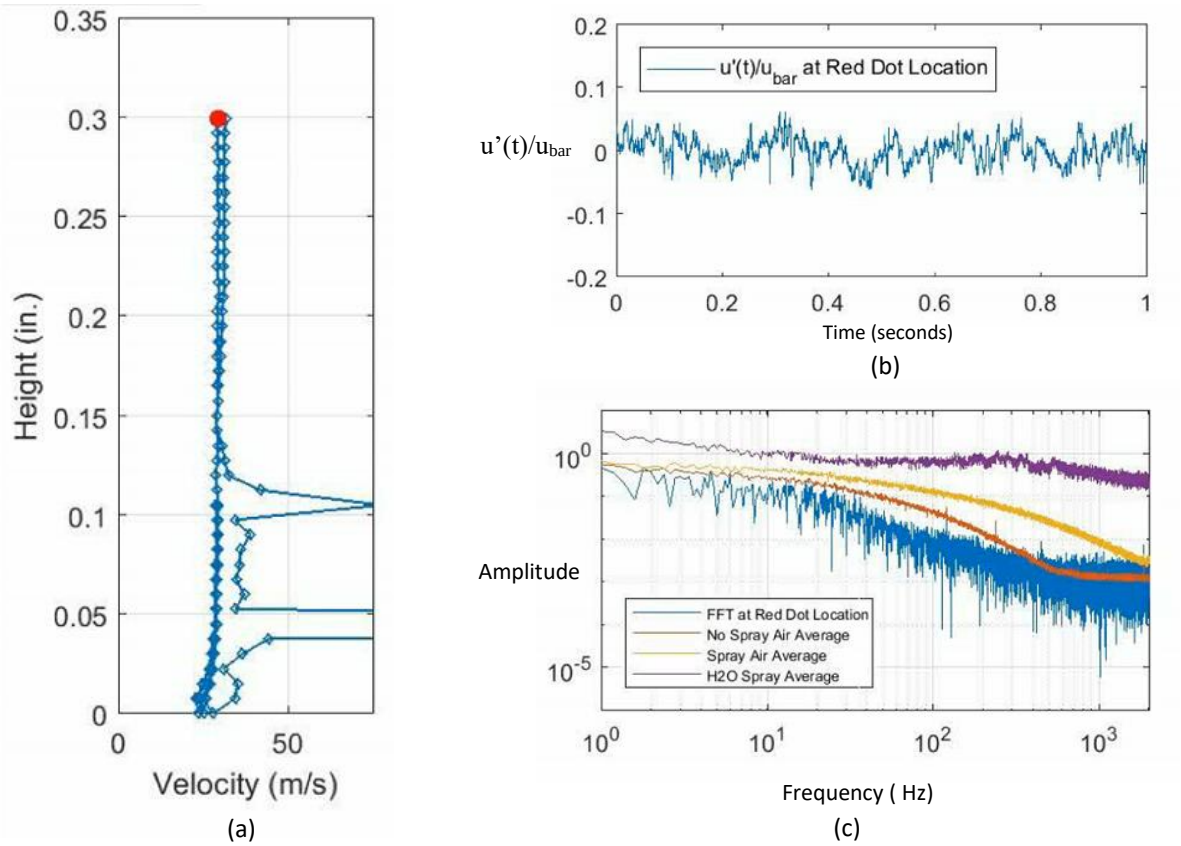

Fig. 15 Hot Wire Outside the Boundary Layer with Nozzle Air and Water Off, Run 091919.01, Velocity = 40 ft/sec (12.2 m/sec)

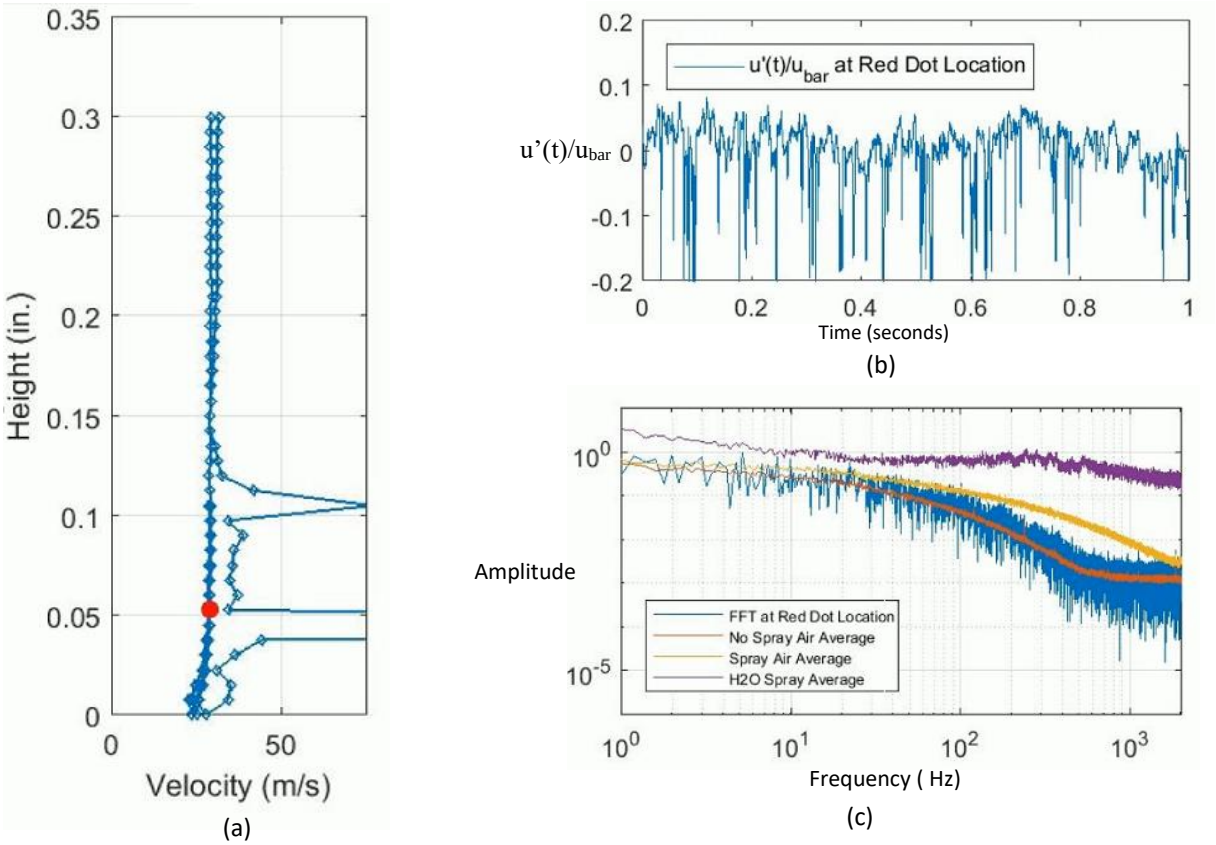

Fig. 16 Hot Wire after traversing the Boundary Layer with Nozzle Air and Water Off, Run 091919.01, Velocity = 40 ft/sec (12.2 m/sec)

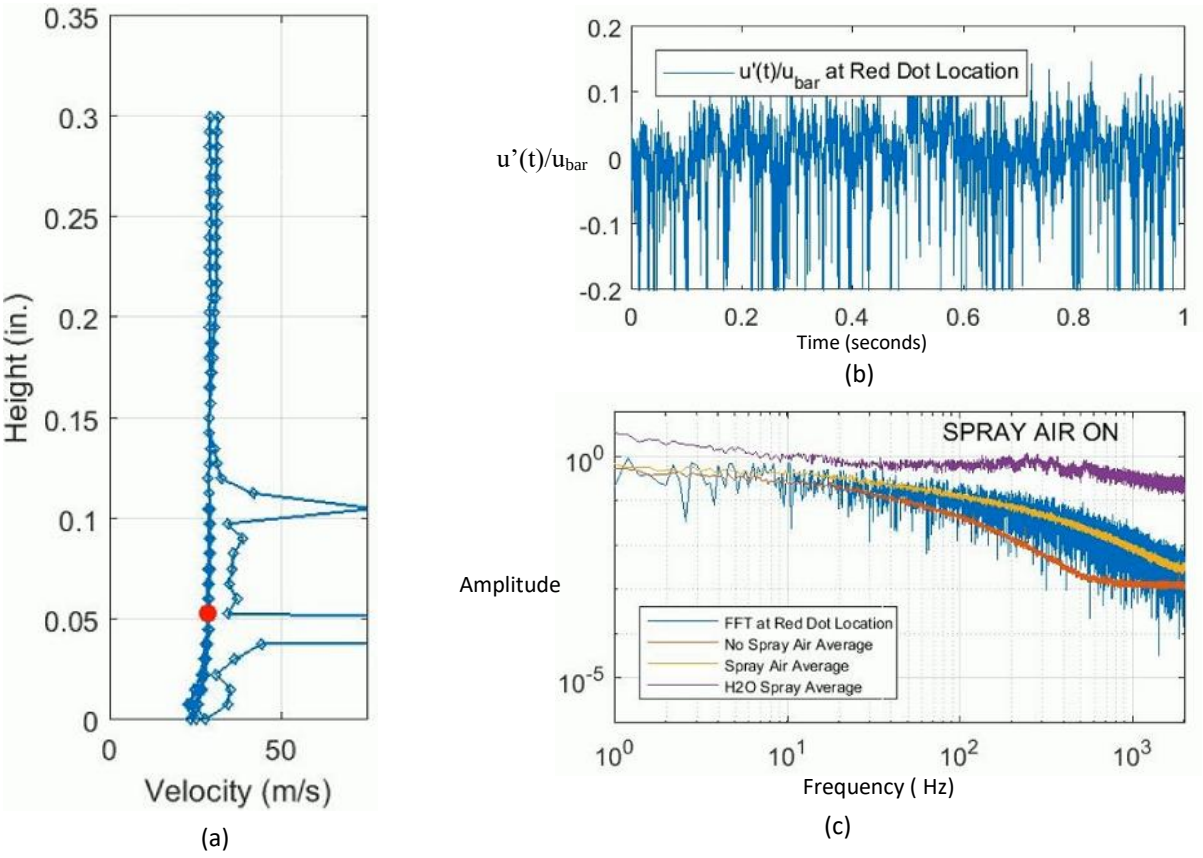

Fig. 17 Hot Wire after traversing the Boundary Layer with Nozzle Air On, Run 091919.01, Velocity = 40 ft/sec (12.2 m/sec)

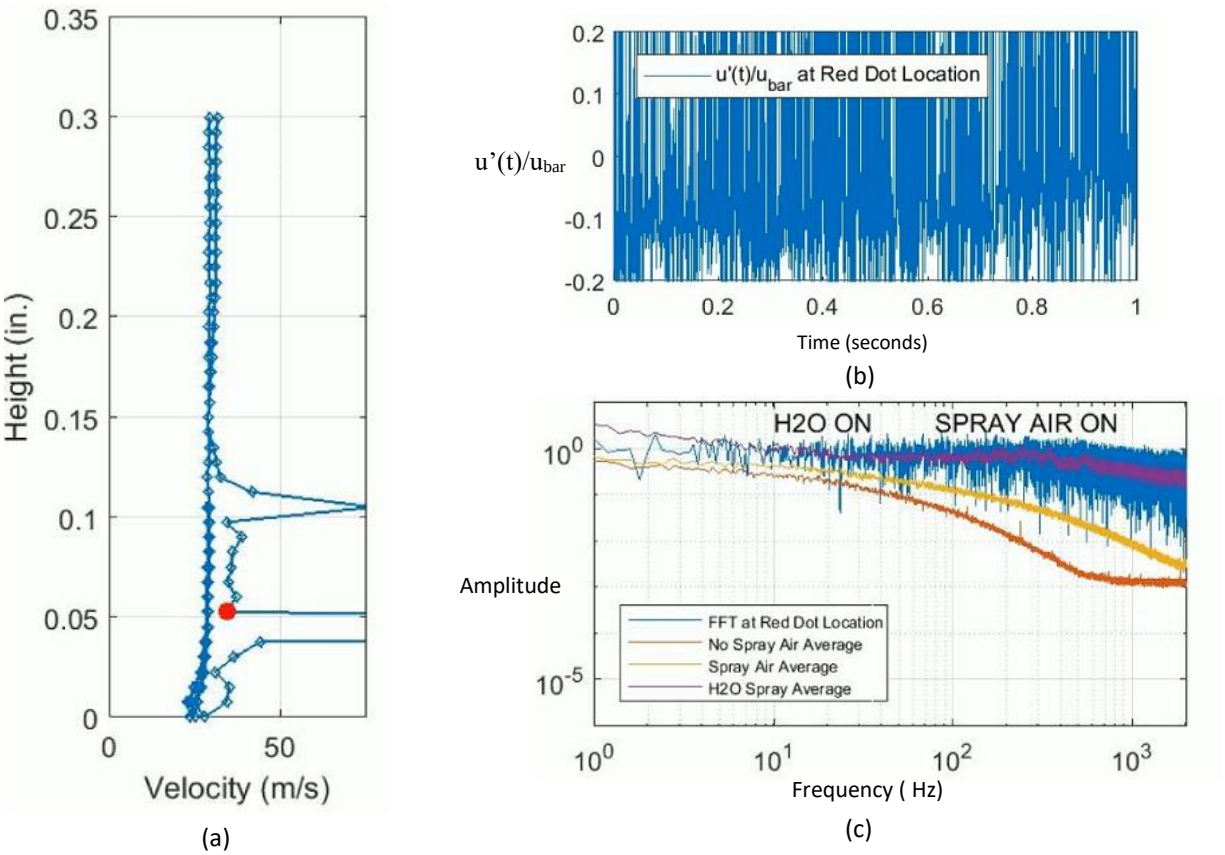

Fig.18 Hot Wire after traversing the Boundary Layer with Nozzle Air and Water On, Run 091919.01, Velocity = 40 ft/sec (12.2 m/sec)

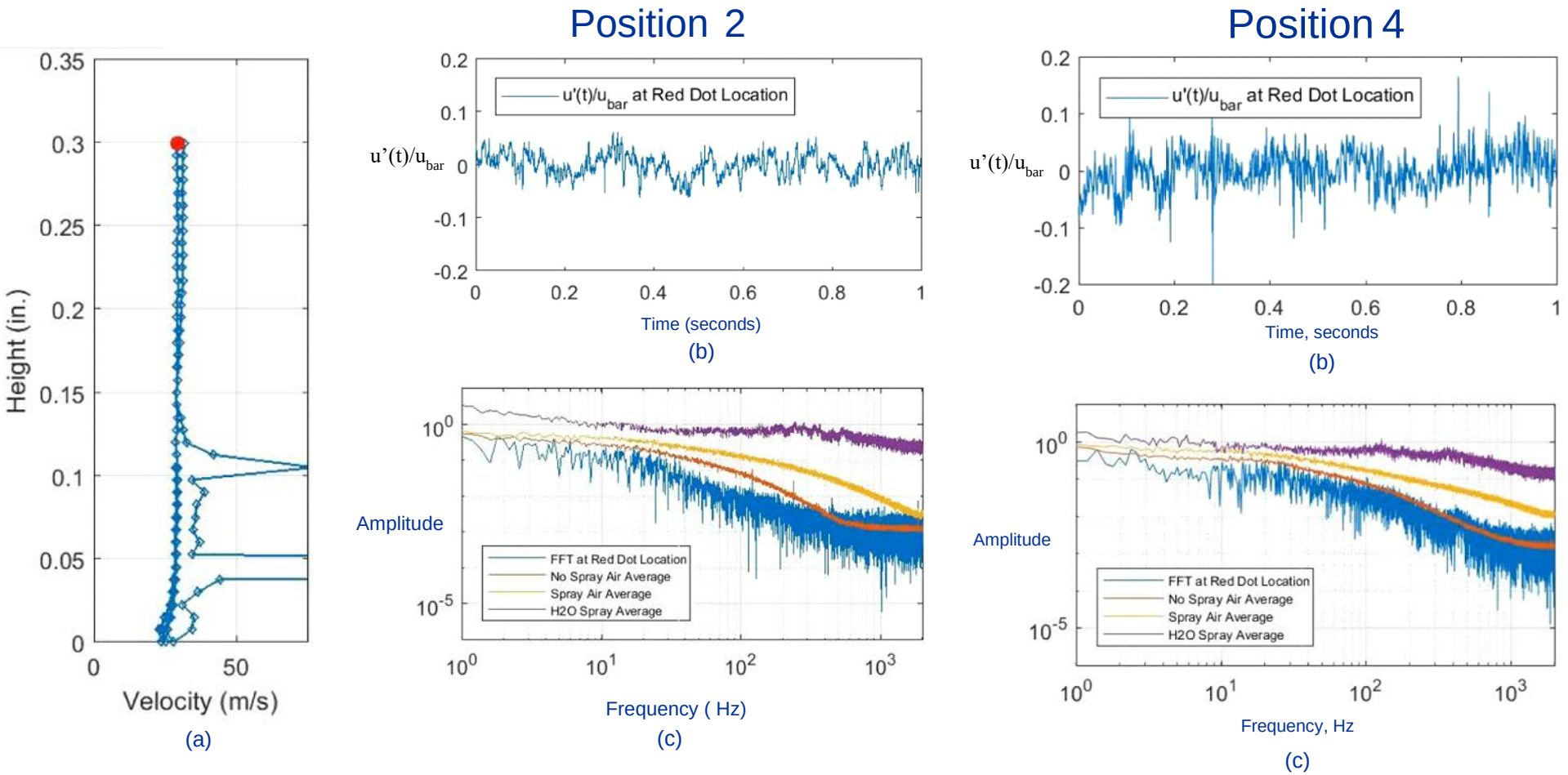

Fig. 19 Comparison between Positions 2 and 4.
Hot Wire Outside the Boundary Layer with Nozzle Air and Water Off
Runs 091919.01 and 091819.04; Velocity = 40 ft/sec (12.2 m/sec)

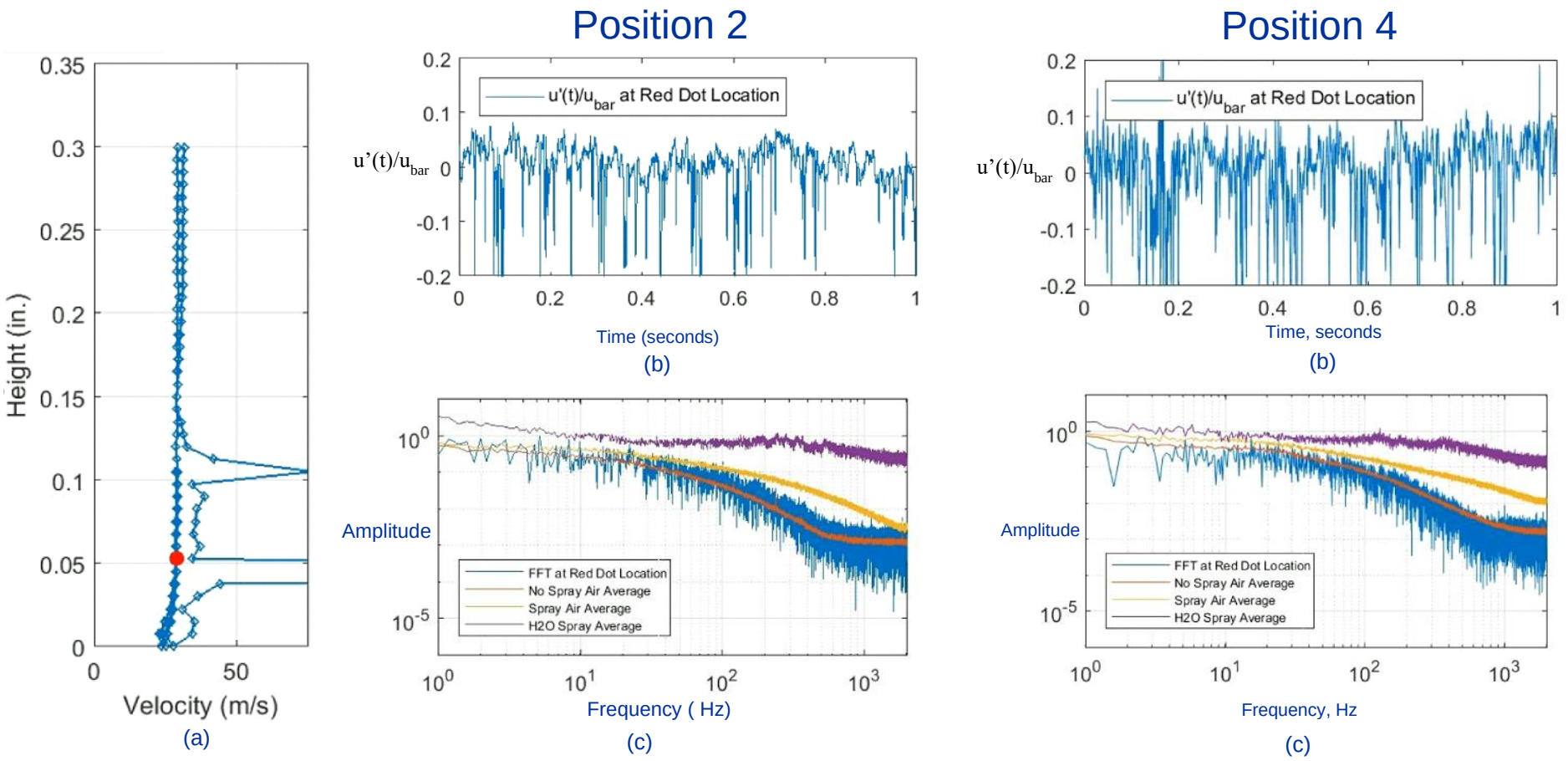

Fig. 20 Comparison between Positions 2 and 4.
Hot Wire after traversing the Boundary Layer with Nozzle Air and Water Off
Runs 091919.01 and 091819.04; Velocity = 40 ft/sec (12.2 m/sec)

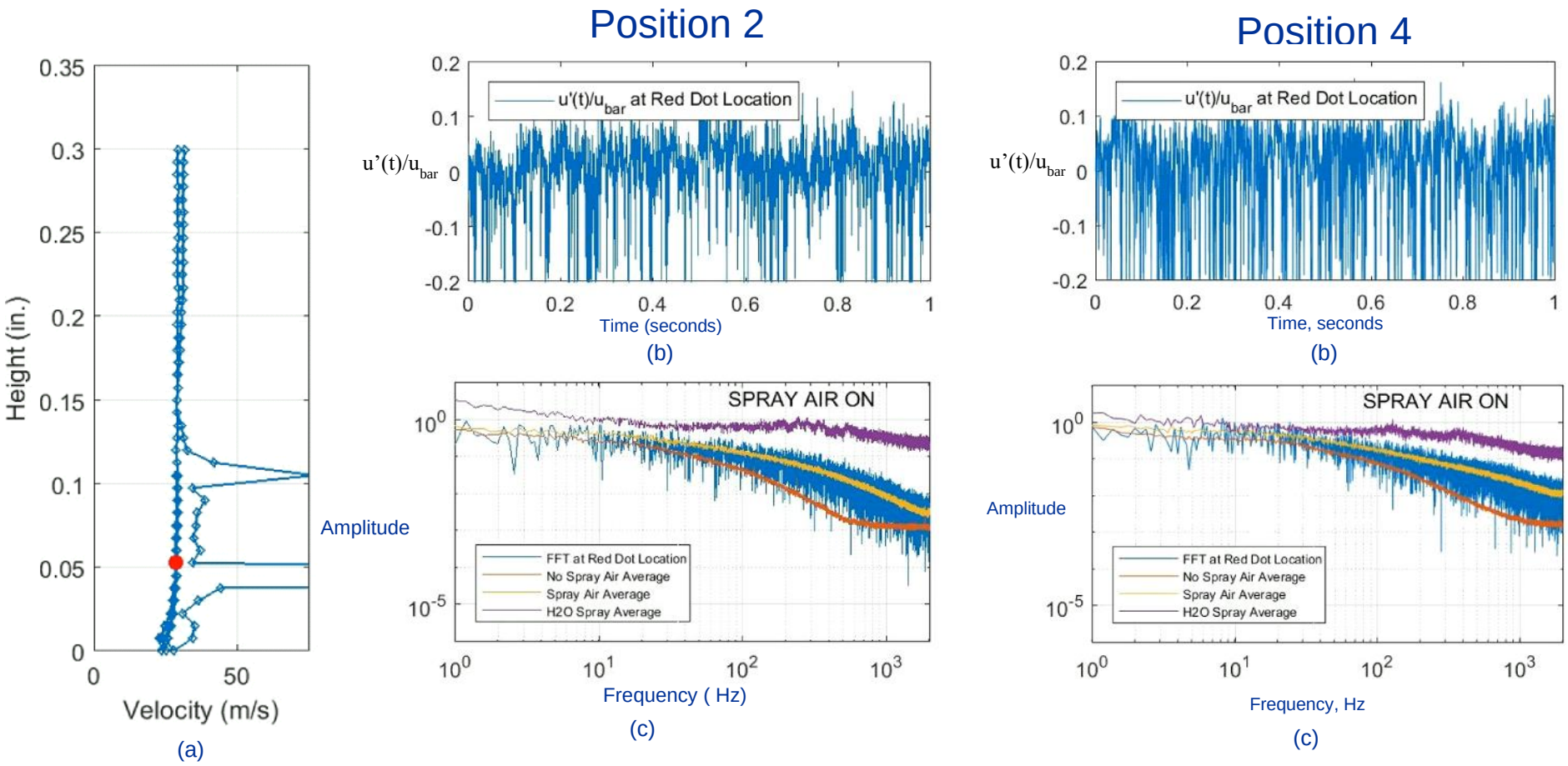

Fig. 21 Comparison between Positions 2 and 4.
Hot Wire after traversing the Boundary Layer with Nozzle Air On
Runs 091919.01 and 091819.04; Velocity = 40 ft/sec (12.2 m/sec)

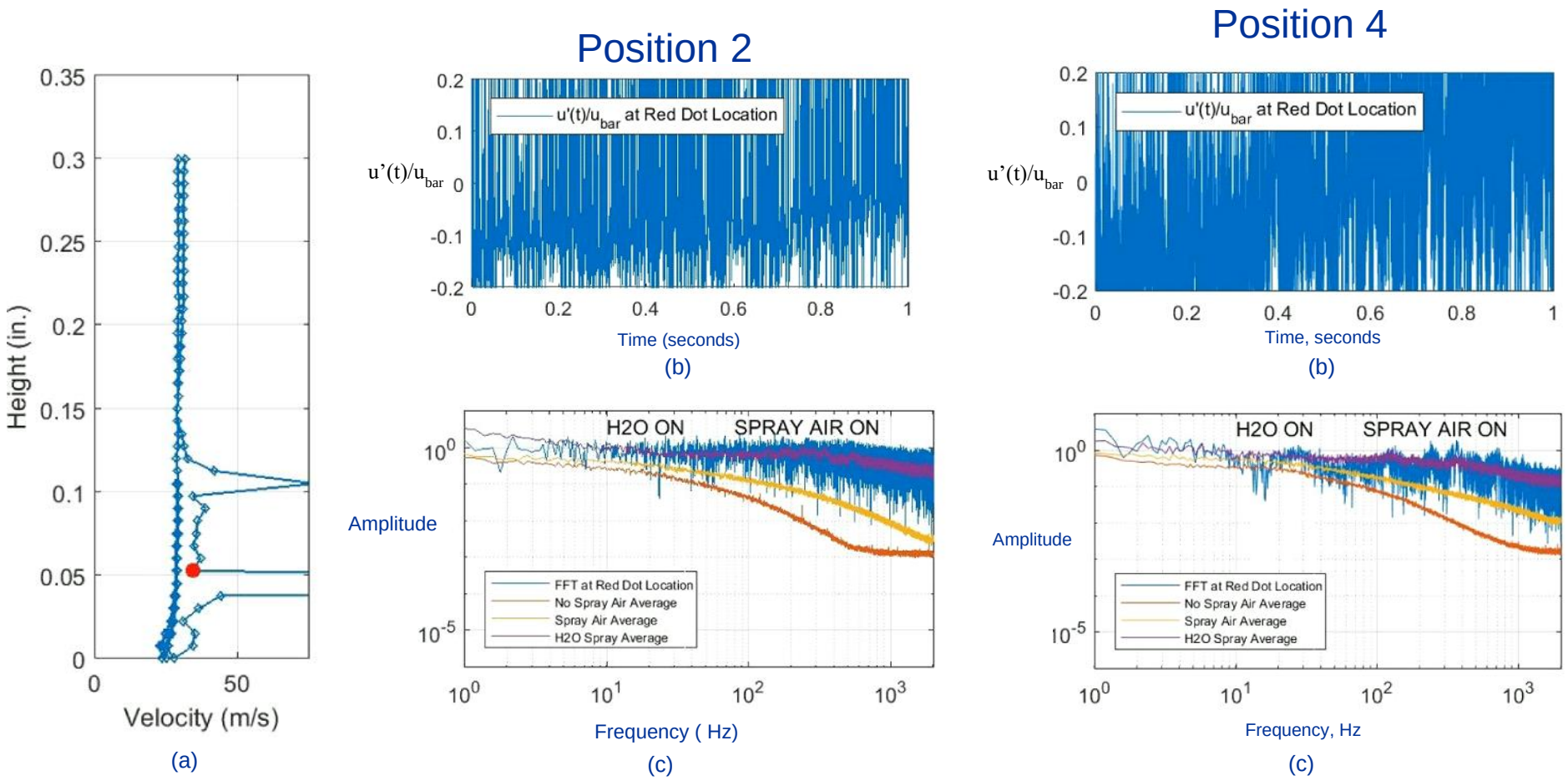

Fig.22 Comparison between Positions 2 and 4.
Hot Wire after traversing the Boundary Layer with Nozzle Air and Water On
Runs 091919.01 and 091819.04; Velocity = 40 ft/sec (12.2 m/sec)

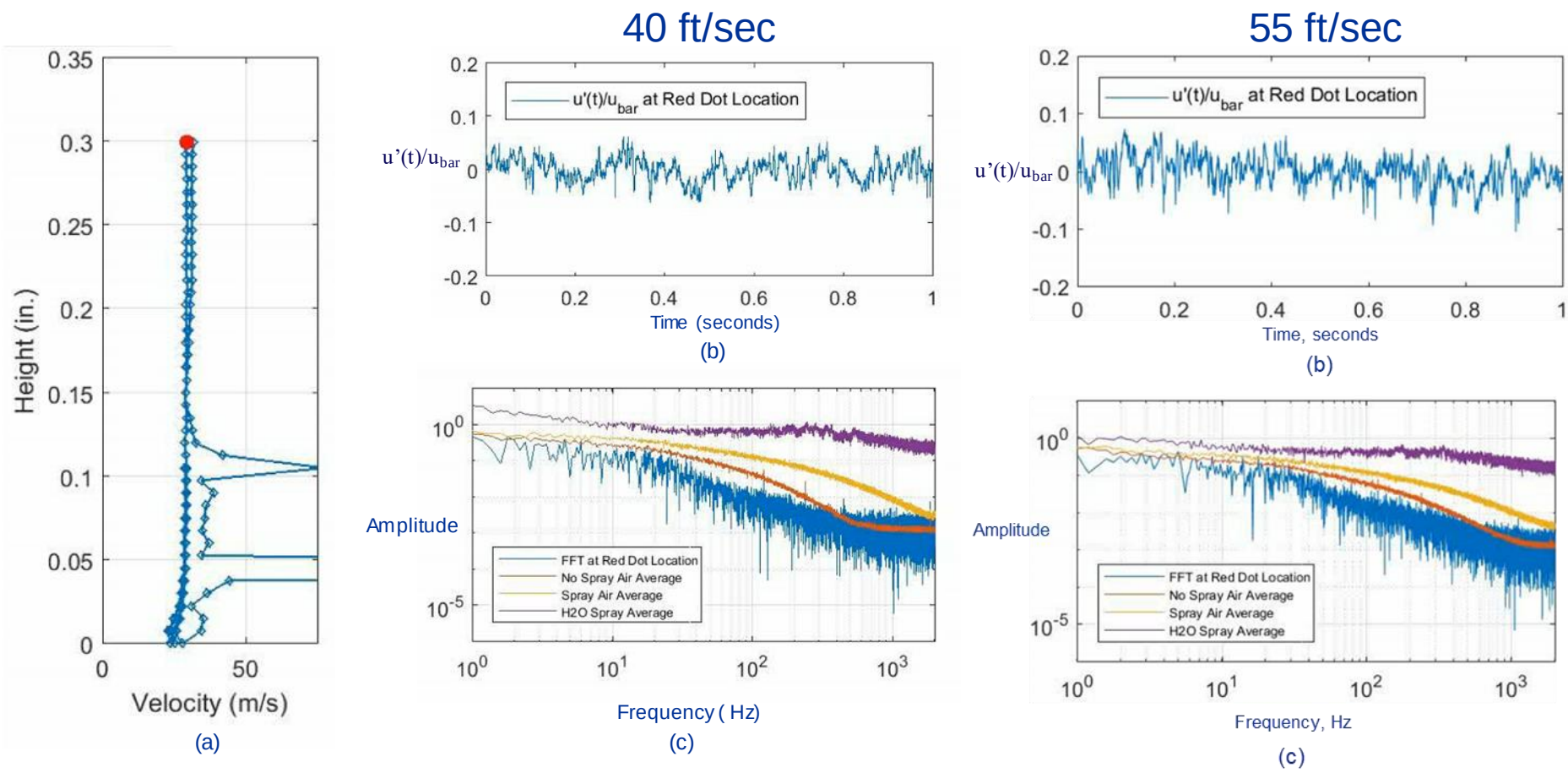

Fig.23 Comparison between Velocities at Position 2.
Hot Wire Outside the Boundary Layer with Nozzle Air and Water Off
Run 091919.01, Velocity = 40 ft/sec (12.2 m/sec)
Run 091819.06, Velocity = 55 ft/sec (15.2 m/sec)

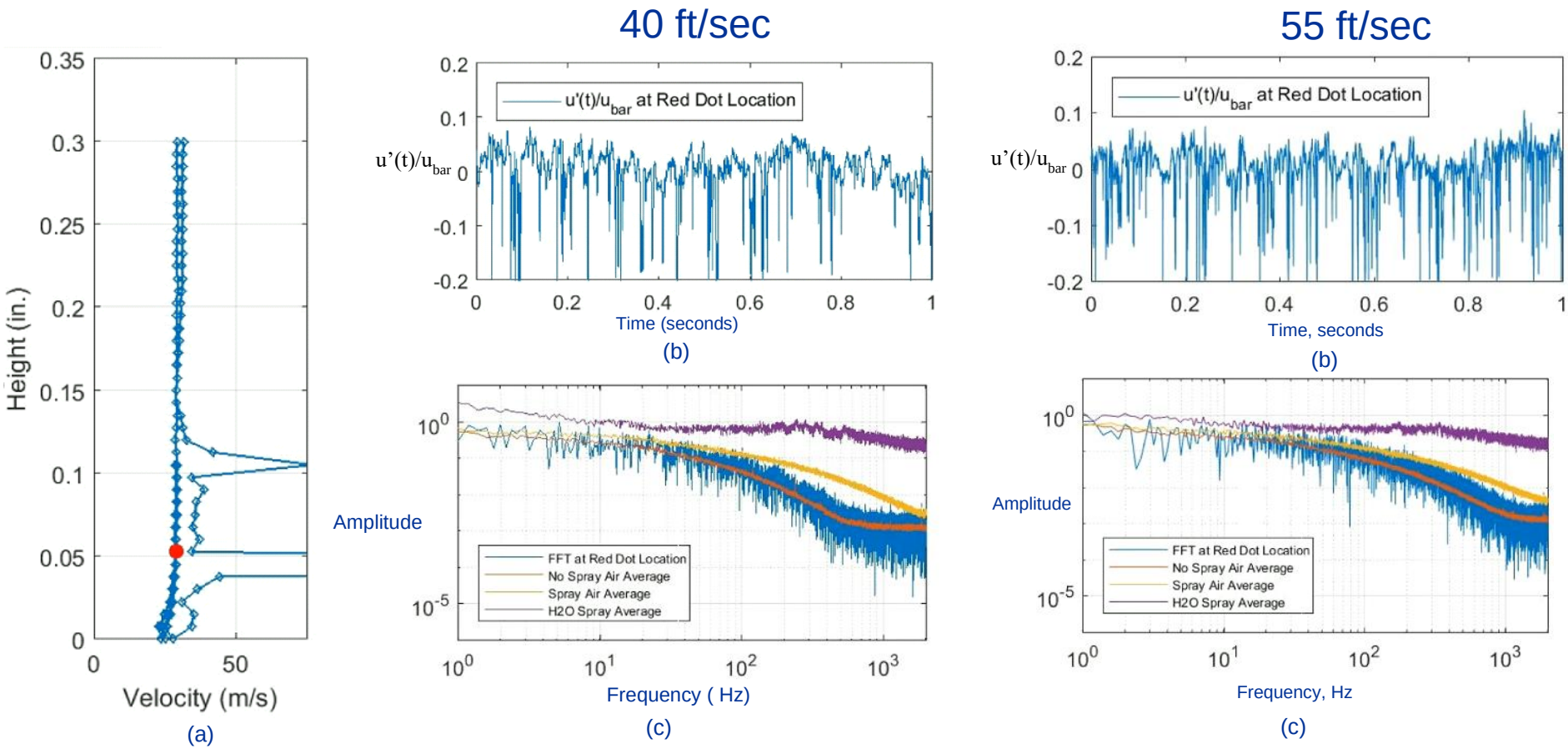

Fig.24 Comparison between Velocities at Position 2.
Hot Wire after traversing the Boundary Layer with Nozzle Air and Water Off
Run 091919.01, Velocity = 40 ft/sec (12.2 m/sec)
Run 091819.06, Velocity = 55 ft/sec (15.2 m/sec)

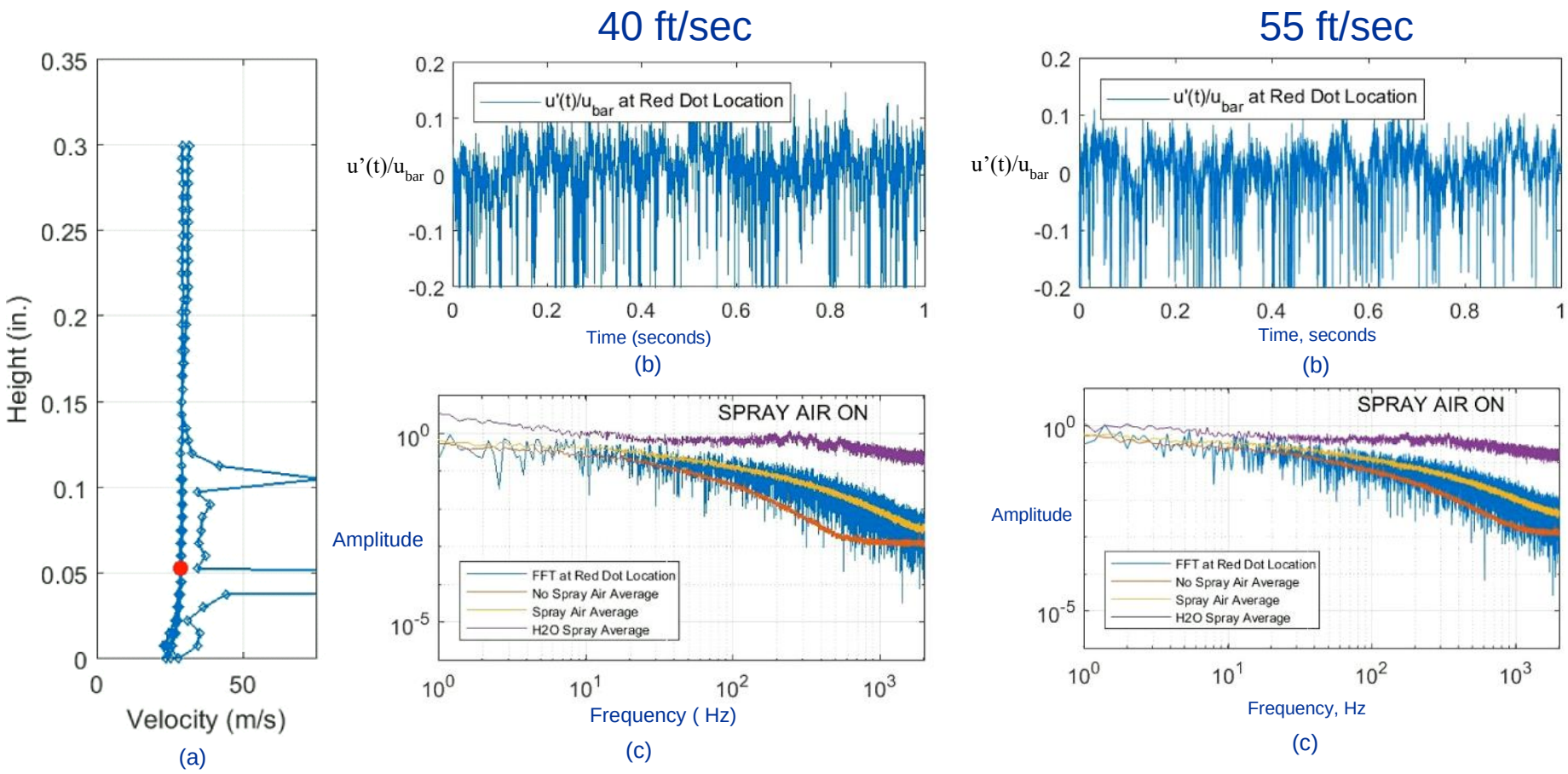

Fig.25 Comparison between Velocities at Position 2.
Hot Wire after traversing the Boundary Layer with Nozzle Air On
Run 091919.01, Velocity = 40 ft/sec (12.2 m/sec)
Run 091819.06, Velocity = 55 ft/sec (15.2 m/sec)

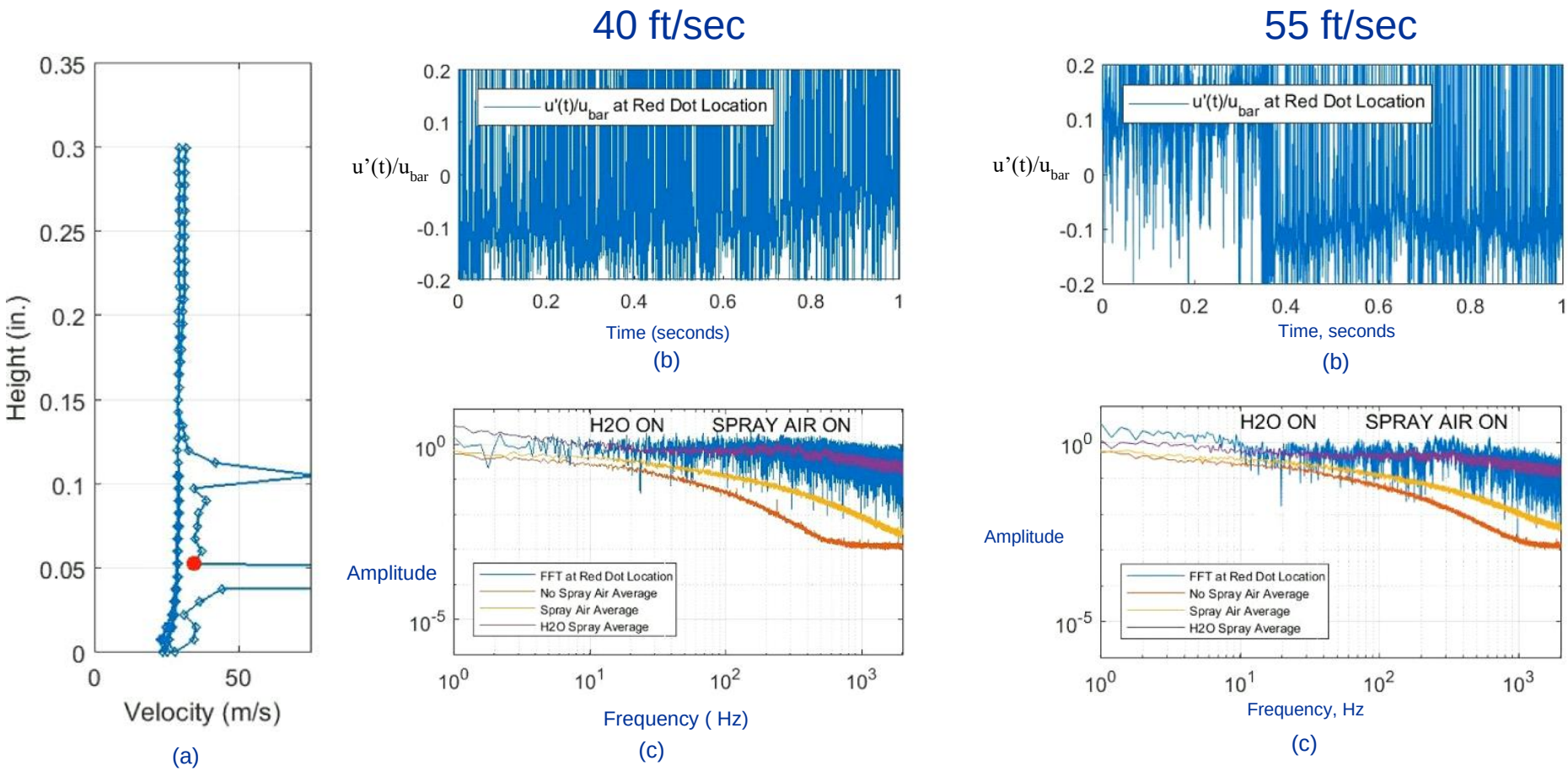

Fig.26 Comparison between Velocities at Position 2.
Hot Wire after traversing the Boundary Layer with Nozzle Air and Water On
Run 091919.01, Velocity = 40 ft/sec (12.2 m/sec)
Run 091819.06, Velocity = 55 ft/sec (15.2 m/sec)